applied sciences

Article

Analysis of Biomechanical Characteristics of External Fixators with Steel and Composite Frames during Anterior–Posterior Bending

Nedim Pervan *, Elmedin Mešić, Adis J. Muminović, Enis Muratović and Muamer Delić

Department of Mechanical Design, Faculty of Mechanical Engineering, University of Sarajevo, 71000 Sarajevo, Bosnia and Herzegovina; mesic@mef.unsa.ba (E.M.); adis.muminovic@mef.unsa.ba (A.J.M.); muratovic@mef.unsa.ba (E.M.); delic@mef.unsa.ba (M.D.)

* Correspondence: pervan@mef.unsa.ba

Abstract: This paper presents a comparative analysis of the biomechanical characteristics of an external fixator with a frame made of two different materials (stainless steel and composite material) during anterior–posterior bending. Before the test itself, two representative configurations of the Sarafix fixator were selected for application on the lower leg and upper extremities under the designations B50 and C50, which are most widely used in orthopedic practice. The examination of the biomechanical characteristics of the external fixator was carried out using the structural analysis of the construction performance of the Sarafix fixator using the finite element method, the results of which were verified through experimental tests. The developed experimental and FEM models study the movement of the fracture crack and enable the determination of the stiffness of structural designs as well as the control of the generated stresses at the characteristic locations of the fixator. The results show that the fixator with a carbon frame has lower stresses at critical points in the construction compared to the fixator with a steel frame, in the amount of up to 49% (at the measuring point MT+) or up to 46% (at the measuring point MT−) for both fixture test configurations. The fixator with a carbon frame has greater displacements at the fracture site compared to the fixator with a steel frame, in the amount of up to 45% (for configuration B50) or up to 31% (for configuration C50). The stiffness of the structure for both test configurations of the fixator is lower in the fixator with a carbon frame compared to the fixator with a steel frame by up to 27%. Based on the findings of this study, we can conclude that a fixator with a steel frame has better biomechanical characteristics compared to a carbon frame.

Keywords: external fixation; stainless steel; composite materials; structural rigidity; fracture rigidity; principal stresses; von Mises stress

check for updates

Citation: Pervan, N.; Mešić, E.; Muminović, A.J.; Muratović, E.; Delić, M. Analysis of Biomechanical Characteristics of External Fixators with Steel and Composite Frames during Anterior–Posterior Bending. *Appl. Sci.* **2023**, *13*, 8621. https://doi.org/10.3390/app13158621

Academic Editor: Anthony William Coleman

Received: 6 June 2023
Revised: 27 June 2023
Accepted: 30 June 2023
Published: 26 July 2023

1. Introduction

Within the framework of biomechanical research on external fixators, great attention is paid to examining the structural parameters influencing the stability of the fixator, such as the rigidity of the fixator, the value of the maximum von Mises stresses at controlled points in the system, and the bearing capacity of the pin–bone connection. Numerous experimental biomechanical studies of different types of fixators have been performed. Remiger [1] experimentally investigates and compares the mechanical properties of a pinless external fixator applied to the lower leg with AO tubular and Ultra-x fixators. The study concludes that AO tubular fixators outperform the other two fixators in terms of stability under all test loads. Grubor et al. [2] compare the biomechanical properties of four external fixators: Ortofix, the M20 fixator, the Charnley fixator, and the Ilizarov fixator. The results are obtained through the examination of 3D finite element method (FEM) models of the fixators, physical models, and clinical investigations. Yang et al. [3] perform biomechanical tests to analyze the influence of the location and number of pins and needles on the stiffness of the hybrid fixator according to axial load and bending in two planes. Vossoughi et al. [4] analyze the influence of the number of pins and trusses as well as the position of the connectors on the pins on the stiffness of the Hoofmann unilateral, uniplanar fixator. The rigidity of the fixator construction is evaluated according to loads that simulate conditions during normal walking.

In the last few years, researchers, in addition to conducting experimental tests, increasingly use the advantages of 3D modeling and numerical analysis to obtain a more complete picture of the behavior of a fixator and its components during loading. Thus, Radke et al. [5], Meleddu et al. [6], Oh et al. [7], and many others have developed FEM models for biomechanical testing of the analyzed fixators. These models are used to determine the displacement values of bone segments at the fracture site and the stiffness values of the system under observed loads. Additionally, the FEM models provide information on the maximum von Mises stress values at characteristic locations, such as the pin–bone contact and the bone segment interfaces. The results obtained through the finite element analysis are validated through experimental testing of the analyzed fixators. With the development of new biomaterials such as polymers and composites, research into the possibility of their application in orthopedics begins [8–10]. The term composite materials refers to materials made up of two or more components that differ both in chemical composition and other properties. The development of these materials has emerged from the need to achieve higher strength and rigidity while reducing weight in many structures. Essentially, composites consist of a matrix and reinforcing materials (fibers or particles). The matrix, which binds the reinforcing materials together into a unified whole, is typically made of polymer resins (such as epoxy, polyester, phenolic), but can also be ceramic, metal, and other materials. The reinforcing fibers can be glass, carbon, aramid, boron, and other materials, while particles can include wood, stone, and other substances. [11]. Baidya et al. [12] conduct numerical and experimental investigations on the stiffness of the Ilizarov fixator ring made of different materials (steel, aluminum, Kevlar, and carbon), as well as its radiotransparency. Lee et al. [13] perform numerical and experimental tests on the C-ring of the Ilizarov fixator, which is made of a carbon fiber-reinforced composite material. Fu et al. [14] perform numerical investigations on the elastic modulus of implants made from (HA)/epoxy composite reinforced with carbon fibers. Zahra et al. [15] conduct tests on the mechanical properties of a hybrid composite material used for manufacturing bone fracture fixation plates. They develop a new composite material and compare its results with the standard metallic material used for bone fracture fixation plates.

Saidpour [16], in their research, attempts to address the issue posed by bone fixation plates made from conventional metallic materials in the later healing stages of bones, namely the potential occurrence of osteoporosis. They numerically analyze stress distribution in composite plates under various loading conditions.

All commercial fixators that are in use today have gone through biomechanical research before their first application. Biomechanical testing of the Sarafix fixator, due to the wartime circumstances in which it was created, was not performed in terms of an exact assessment of its stability under the loads to which it is exposed during the postoperative period of patient treatment. The basic quantity for stability comparison is the stiffness of the system obtained based on the interfragmentary displacement at the point of fracture and the point of loading. In this work, a biomechanical test of the Sarafix fixator with a frame made of two different materials (stainless steel and composite material) was performed for two different configurations of the fixator (B50 and C50). The main goal of this research is to quantify the mechanical behavior of the standard Sarafix fixator under the influence of anterior–posterior bending for different frame materials, as well as different configurations of the fixator.

2. Development of the External Fixation Model

Before the test itself, two appropriate configurations of the Sarafix fixator that have the greatest application in orthopedic practice were selected. When forming the test configurations, the position of the tibia in the lower leg and other specifics were taken into account. Namely, the tibia in the lower leg is located eccentrically and close to the skin, which has the effect of making this bone extremely exposed to external influences, i.e., injuries and fractures, but at the same time, its specific position facilitates the application of fixators. Two representative configurations of the Sarafix fixator were selected for application on the lower leg and upper extremities under designations B and C (Figure 1).

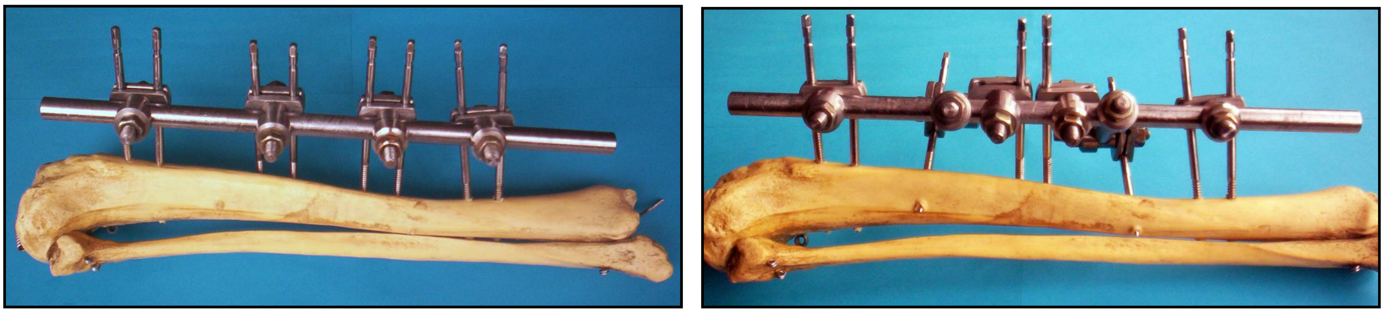

(**a**) (**b**)

Figure 1. Sarafix fixation device with steel frame; (**a**) B50 configuration, (**b**) C50 configuration.

It is important to note that for the test configuration of the fixator, an open bone fracture with a bone structure defect in the value of the interfragmentary gap of 50 mm was simulated. This value was obtained based on data from orthopedic practice and corresponds to the length of an open fracture with a larger bone structure defect [17,18].

Configuration B is a unilateral external fixator consisting of four half-pins placed in the upper and lower segment of the bone (Figure 1a). All half-pins are located in the AP plane parallel to each other. Version B is mainly used on the lower leg and upper extremities. Configuration C is a unilateral biplanar external fixator consisting of four half-pins each placed in the upper and lower segments of the bone (Figure 1b). Unlike version B, it has one half-pin each in the upper and lower segments placed in a plane that overlaps with an angle of 45° in relation to the AP plane. In this way, the half-pins are arranged in two planes and, together with the other components, form one so-called triangular or delta construction, which achieves biplanar stiffening of bone segments. During the development of the device for external fixation (Sarafix with a frame made of composite material) care was taken to ensure that it geometrically and dimensionally corresponds to the original device (frame made of stainless steel) in order to be able to compare the obtained results. Additionally, when choosing the composite material, it was taken into account that it should be the material that is most often used today in the manufacture of fixators, which is a composite material reinforced with carbon fibers. The mechanical characteristics of the composite material used in the manufacture of the fixator frame are shown in Table 1.

Table 1. Mechanical properties of the composite material Std-CF-UD and beech wood [1,19].

Property	**Mark**	**Std-CF-UD**	**Beech Wood**
		Value	
Longitudinal tensile strength	X_t	1500 MPa	135 MPa
Transversal tensile strength	Y_t	50 MPa	2.8 MPa
Longitudinal compressive strength	X_c	1200 MPa	60 MPa
Transversal compressive strength	Y_c	250 MPa	13 MPa
Longitudinal flexural strength	X_S	1200 MPa	148 MPa
Ultimate in-plane shear strength	S	70 MPa	8.5 MPa
Longitudinal modulus of elasticity	E_L, E_{11}	135 GPa	15.4 GPa
Transversal modulus of elasticity	E_T, E_{22}	10 GPa	1.12 GPa
Poisson's ratio	ν_{12}	0.3	0.66
Shear modulus	G_{12}	5 GPa	0.45 GPa
Density	ρ	1600 kg/m^3	740 kg/m^3

Before performing the tests, it was necessary to create human bone models on which the Sarafix external fixation system versions would be placed. Different materials are used to make human bone models. The most commonly used materials are PVC, wood, aluminum, copper, etc. In these studies, a simplified model of the human lower leg bone made of beech wood, with known mechanical characteristics similar to human bone, was used (Table 1) [20,21]. The final appearance of the Sarafix fixator with a frame made of composite material applied to bone models made of beech wood is given in Figure 2.

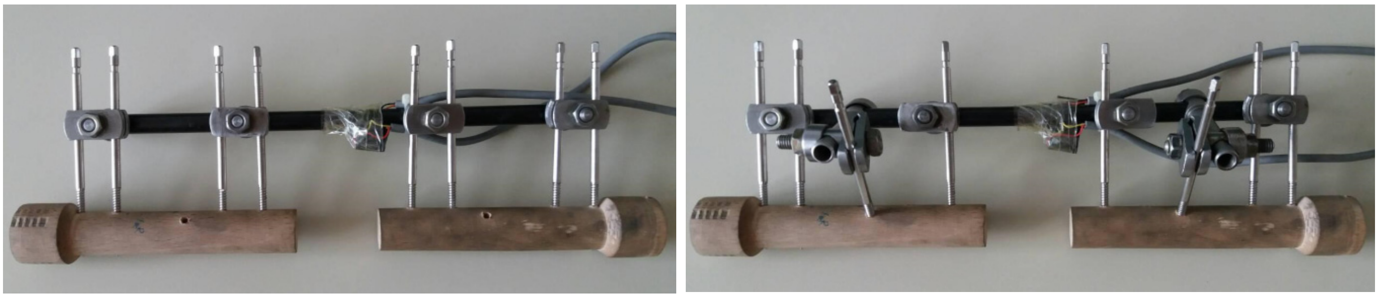

(a) (b)

Figure 2. Sarafix fixation device with composite frame; (**a**) B50 configuration, (**b**) C50 configuration.

3. Finite Element Model and Structural Analysis of Fixators

Modeling a structure is the creation of an idealized and simplified presentation of the behavior of a structure exposed to various actions. This is a key step in analysis and design because errors and omissions in modeling can cause problems in the functioning of the structural system. The formulation of the model implies the choice of geometric, physical, mathematical, and, finally, numerical approximation of the phenomenon. The goals of practical (not only qualitative) analysis limit the number of possible models. There is always a dilemma when choosing a model, because more complex models are more accurate, but at the same time, less efficient. The fixator and bone model are discretized with linear (TE4) and parabolic (TE10) tetrahedron finite elements. A linear tetrahedron contains four nodes at the vertices and has a total of twelve degrees of freedom. A parabolic tetrahedron is a form of a curvilinear tetrahedron with ten nodes and a linear change of deformations within the element. The FEM model of the fixator is discretized with 120,953 TE4 finite elements (46.7%) and with 109,816 TE10 finite elements (42.4%). Both elements belong to the group of 3D isoparametric elements, i.e., solids with six edges. With isoparametric elements, the same interpolation functions and the same nodes are used to approximate their geometry and the field of basic unknowns in the element. In each node of these finite elements, there are three degrees of freedom (displacement). Connections between individual parts of the fixator structure (solid, contact, and screw connections) as well as connections for modeling the influence of the supports (sliding connection) were modeled with spider-type elements (28,232 finite elements or 10.9%). In this way, the FEM model of the fixator consists of a total of 259,001 finite elements with 262,652 nodes, which results in 787,959 degrees of freedom (number of DOF), (Figure 3). For the production of medical devices, the device from Figure 1 is completely made of stainless steel, which is modeled as an isotropic linear elastic material in the FEM analysis. In the case of isotropic materials, the constitutive relations, that is, the stress–strain relations, contain only two constants: the modulus of elasticity and Poisson's ratio, which, for the given steel, have the values E = 215 GPa and ν = 0.29, respectively. The device from Figure 2 is made of stainless steel (couplings, coupling carrier, and half-pins) and composite material (fixator frame). For steel, we have already noted that in the FEM analysis, it is modeled as an isotropic linear elastic material, while the composite material is modeled as an anisotropic material, and thanks to the cylindrical symmetry of its structure, it can be viewed as an orthotropic material where the properties are defined in three planes determined with transverse, tangential, and the radial section of the frame. The models of bone segments are made of beech wood, which has known mechanical characteristics (Table 1). Wood belongs to the group of anisotropic materials, but thanks to the cylindrical symmetry of its structure, it can be viewed as an orthotropic material where the properties are defined in three planes determined by the transverse, tangential, and radial cross-section of the trunk. A small rectangular segment with three axes of symmetry, longitudinal (L), radial (R), and tangential (T), can be distinguished from the truss, which are approximately perpendicular to each other.

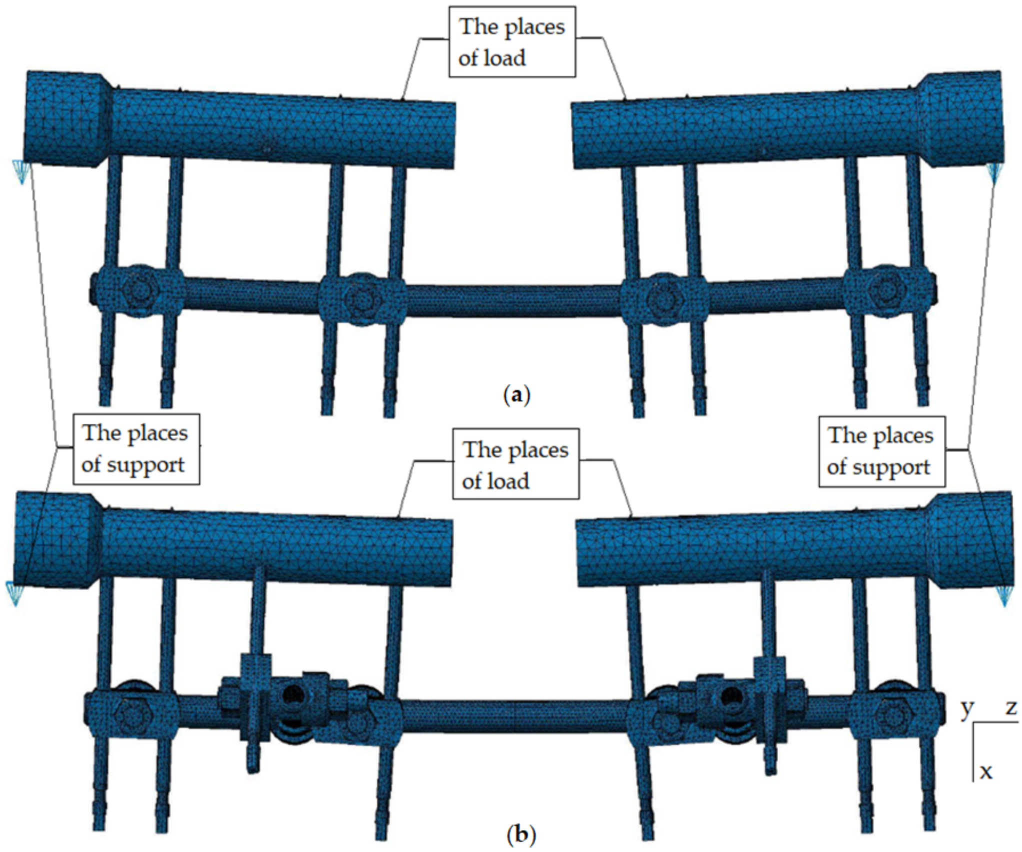

Figure 3. FEM model of the Sarafix device—preprocessing; (**a**) B50 configuration, (**b**) C50 configuration.

For the composite material and the material of the bone segment model, which is modeled as a 3D orthotropic linear elastic material in FEM analysis, it is common to define material parameters such as the modulus of elasticity, Poisson's ratio, and slip modulus (Table 1). During application, the fixator is exposed to a complex load that is a combination of pressure, bending, and twisting. In most studies of external fixation devices, using the finite element method and/or experimental tests, separate tests are performed on axial load with compressive force and sagittal or anterior–posterior (AP) bending and twisting [22,23]. In this study, the external fixation device was tested for anterior–posterior bending. An FEM model was developed that simulates an experimental test on anterior–posterior bending, taking into account the complete geometry of the fixator and the bone model, the connections between the components, the applied load, and the applied restrictions. The structural analysis of AP bending of the FEM model of the Sarafix fixator prototype was performed by making two flat surfaces for support on the models of the upper and lower segment of the bone, i.e., the cylindrical bone models were leveled at the places of support. The support is achieved by utilizing contact with virtual parts attached to the flat surfaces on the bone segment models (Figure 3).

The structural bending analysis of the fixator model was performed with a concentrated load at the fracture site, the maximum value of which was 500 N, i.e., 250 N at both ends of the bone model segment symmetrically. To prevent the movement of the model in space, three translations are prevented on one of the support surfaces on the bone model segment, while two translations are prevented on the other bone segment model. The load intensity corresponds to the physiological load of the fixator after its application in the patient and is defined based on the results of in vivo tests [7,24]. The structural analysis was carried out with the following assumptions concerning the actual situation: the load is quasi-static, the support is modeled with appropriate frictionless joints and supports, the connection between the half-pins and the bone is solid, and the characteristics of the material for the bone model correspond to the mechanical characteristics of beech wood. During the structural analysis, the displacement values at the point of loading were monitored (Figure 4), based on which the stiffness of the fixator structure is defined as the relationship between the load and the displacement of the bone at the point of impact of the load. The stiffness of the fixator structure according to AP bending (Cp) is calculated using the following relation [25]:

$$C_s = \frac{F_s}{\delta_s} \left[\frac{\mathrm{N}}{\mathrm{mm}}\right] \tag{1}$$

where F_s is the bending force (N) and δ_s is the deflection due to load (mm).

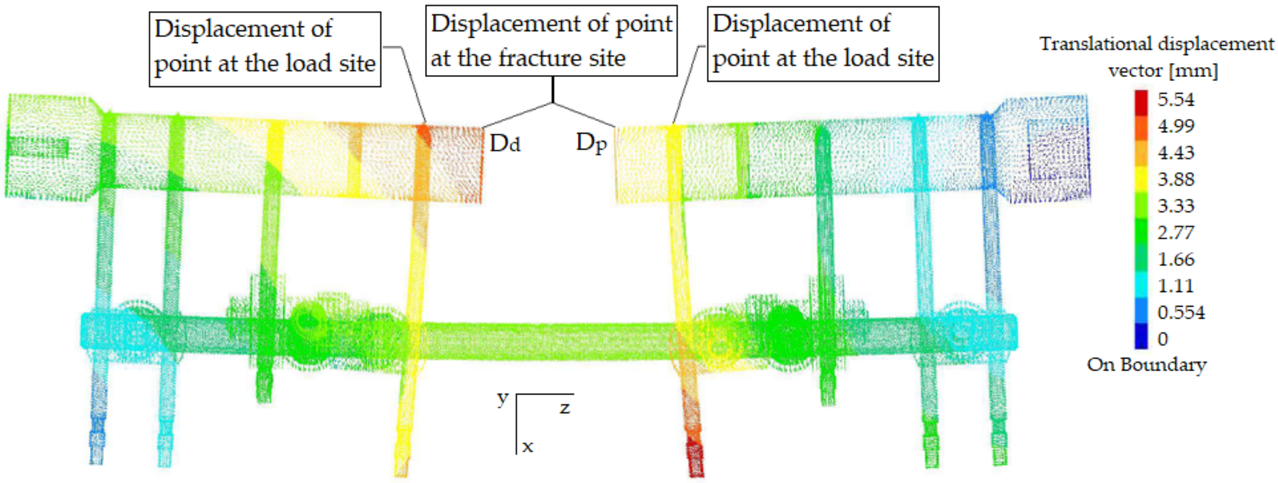

Figure 4. FEM model of the Sarafix device (C50)—postprocessing.

When defining fracture stiffness, displacements in the x, y, and z direction of a pair of adjacent points on the end planes of the proximal (upper) and distal (lower) segment of the bone model at the fracture site were determined, for which the vector of the resulting relative displacement (R) has a maximum value. The intensity of the maximum interfragmentary displacement vector at the fracture site R is defined by [26]:

$$R = \sqrt{\left(r_{D(x)}\right)^2 + \left(r_{D(y)}\right)^2 + \left(r_{D(z)}\right)^2} \tag{2}$$

The relative displacements of a pair of observed points on the end planes of the proximal (upper) and distal (lower) segments of the bone model in the x, y, and z directions are determined as [27]:

$$\begin{aligned} r_{D(x)} &= D_{p(x)} - D_{d(x)} \\ r_{D(y)} &= D_{p(y)} - D_{d(y)} \\ r_{D(z)} &= D_{p(z)} - D_{d(z)} \end{aligned} \tag{3}$$

where $r_{D(x)}$, $r_{D(y)}$, and $r_{D(z)}$ are the relative displacements of the bone segment points in the x, y, and z directions (mm), $D_{p(x)}$, $D_{p(y)}$, and $D_{p(z)}$ are the displacement of the proximal bone segment in the x, y, and z directions (mm), and $D_{d(x)}$, $D_{d(y)}$, and $D_{d(z)}$ are the displacement of the distal bone segment in the x, y, and z directions (mm).

Fracture stiffness is determined as the relationship between the load and the resulting maximum interfragmentary (relative) displacement of the bone segments [28]:

$$C_{ps} = \frac{F_s}{R_{max}} = \frac{F_s}{\sqrt{\left(r_{D(x)}\right)^2 + \left(r_{D(y)}\right)^2 + \left(r_{D(z)}\right)^2}} \quad (4)$$

Figure 3b shows the FEM model of the fixator of the C50 configuration after preprocessing, while Figure 4 shows the same configuration of the fixator after postprocessing, i.e., moving the points of the structure during AP bending. For the biomechanical studies of the stability of the fixator to be complete, in addition to the analysis of displacement at the fracture site, it is necessary to include the analysis of the main stresses at the characteristic points of the fixator structure [29]. During the structural analysis, when monitoring the displacement values of the characteristic points on the bone models, the values of the main and von Mises stresses were controlled at two places in the middle of the truss. The measurement location closer to the bone model segment is marked with MM−, while the location on the opposite side of the truss is marked with MM+ (Figure 5).

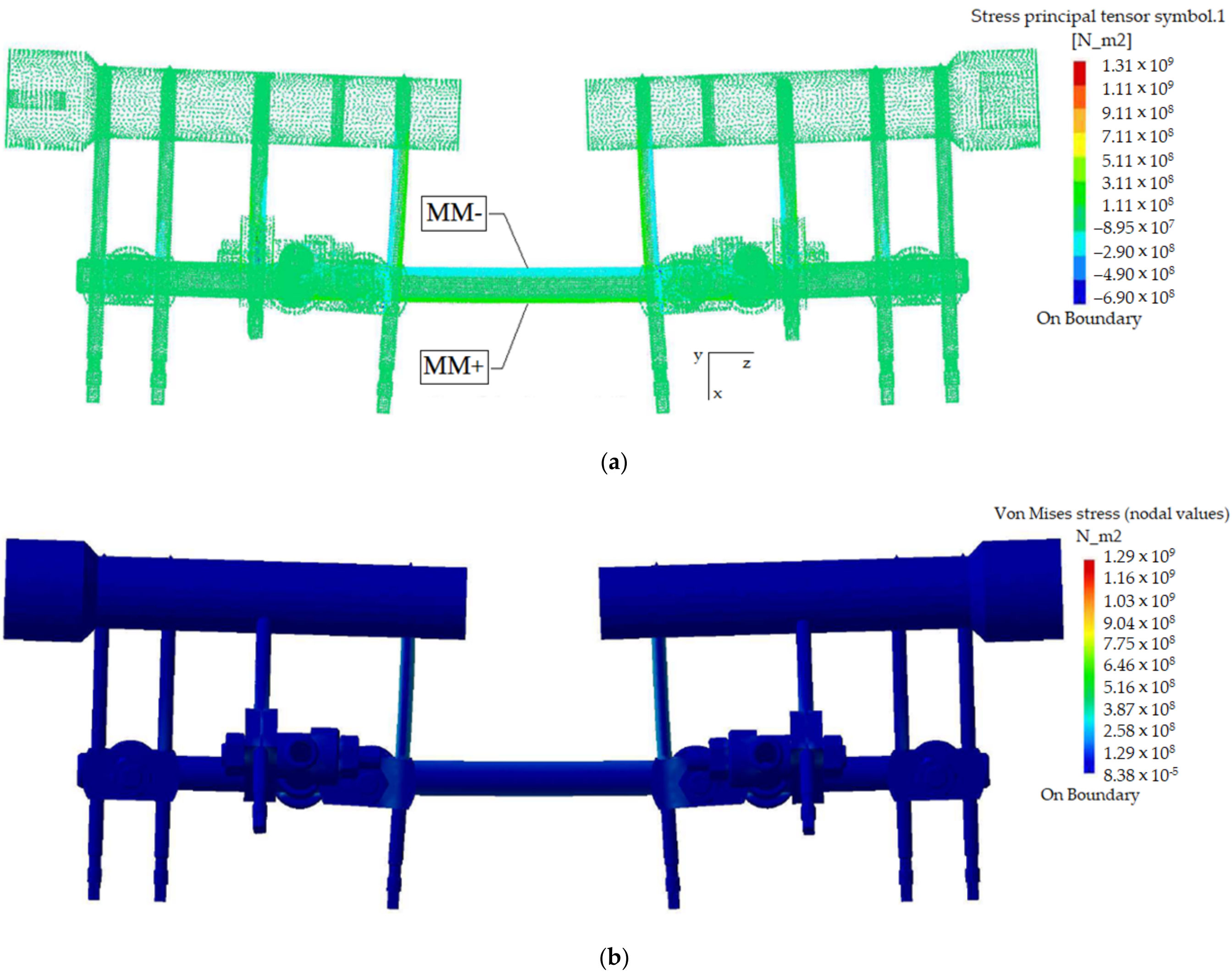

Figure 5. FEM model of the Sarafix device (C50); (**a**) main stresses, (**b**) von Mises stress.

The value of the maximum main stress (σ_1) at the location MM+ is significantly higher (of the order of 10^3) compared to the other two main stresses (σ_2 and σ_3). Based on this, it is obtained that the von Mises stress (σ_{vm}) is equal to the highest principal stress (σ_1) at the location MM+ (Table 2). Also, the value of the minimum main stress (σ_3) at the location MM−, in absolute value, is significantly higher (of the order of 10^3) compared to the other two main stresses (σ_1 and σ_2). Based on this, it is obtained that the von Mises stress (σ_{vm}) is equal to the smallest principal stress (σ_3) at the location MM− (Table 2).

Table 2. Examination results for the Sarafix fixation device.

Configuration	Type of Frame	Type of Test	Displacement at the Load Site, δs, mm	Displacement at the Site of Fracture, Mm						Displacement at the Site of Fracture, R, mm	Structural Rigidity C_S, N/mm	Fracture Rigidity C_{PS}, N/mm	Stress, MPa	
				Proximal Part			Distal Part							
				$D_{p(x)}$	$D_{p(y)}$	$D_{p(z)}$	$D_{d(x)}$	$D_{d(y)}$	$D_{d(z)}$				σ_1, MM+	σ_3, MM−
B50	Carbon	FEM	3.38	3.87	−0.31	−0.69	3.89	−0.42	3.11	3.80	147.93	131.58	147	−154
C50	Carbon	FEM	3.40	3.87	−0.35	−0.67	3.90	−0.56	2.93	3.60	147.06	138.88	149	−154
B50	Steel	FEM	2.47	2.81	0.15	−0.53	2.81	0.15	2.09	2.62	202.43	190.55	284	−284
C50	Steel	FEM	2.48	2.80	−0.03	−0.53	2.80	−0.03	2.21	2.74	201.61	182.22	284	−284
B50	Carbon	Experiment	3.65	3.96	-	−0.48	3.91	-	3.43	-	136.98	-	156	−167
C50	Carbon	Experiment	3.30	3.76	-	−0.61	3.84	-	2.75	-	151.52	-	136	−148
B50	Steel	Experiment	2.48	-	-	-	-	-	-	-	201.61	-	263	−269
C50	Steel	Experiment	2.59	-	-	-	-	-	-	-	193.05	-	-	-

4. Experimental Testing of Fixators

The experimental tests are of the in vitro type (tests on models) and are performed on a material testing machine with the use of appropriate measuring equipment and a device for supporting the model (Figure 6). In real conditions, the fixator is exposed to loads through bone segments and this fact was taken into account, so during the experimental tests, the load of the fixator was carried out by means of bone model segments made of beech wood [30]. One pair of wooden models of the lower leg bones was made in order to simulate an open fracture with a bone structure defect, the inter-fragment distance of which is 50 mm. The surfaces for supporting the wooden models are adapted to the supports on the appropriate devices for their acceptance. After assembling the tested designs of the Sarafix fixator for bone models, they were placed on the material testing machine (Figure 6). In this way, the load is transferred from the bone model to the fixator, corresponding to the actual condition. The value of the tightening torque of the screw connections has a significant influence on the mechanical characteristics of the fastener. Here, it is important to know the minimum value of the tightening torque that will prevent the clamping connections from slipping. If one or more connections slip, the stability of the entire system is impaired, i.e., the load–displacement connection is no longer linear. For these reasons, before starting the test, all screw connections on the Sarafix External Fixation System versions were tightened with a calibrated torque wrench. The tightening torque is 20 Nm.

Figure 6. Experimental setup: 1—displacement transducer; 2—force transducer; 3—light source; 4—distal part of the bone model; 5—proximal part of the bone model; 6—support device; 7—digital high-speed CMOS camera.

The loading of test configurations of the Sarafix fixator was carried out over the tops of two half-pins located on the upper and lower segments of the bone model closest to the fracture site (Figure 6). The bending load was performed in the interval 0–500 N with a force change rate of 2 N/s. The unloading of the fixator structures from 500–0 N was also performed with the same rate of change in the load value. The load intensity is controlled by means of a force transducer on the material testing machine. The support device contains two horizontally placed cylinders on which the segments of the bone model are supported. The distance between the central axes of the cylinders is 362 mm (Figure 6).

During the test, the movement at the load point was monitored through a displacement sensor, and the load was controlled employing a force sensor (type U2A manufactured by HBM—Hottinger Baldwin Messtechnik GmbH, Darmstadt, Germany) on a material testing machine (Zwick GmbH & Co., Ulm, Germany, model 143501). On the other hand, the displacements of the bone model segments at the fracture site were monitored utilizing a digital high-speed CMOS camera (PCO AG, type: pco.1200 s, Kelheim, Germany) (Figure 6). Stress analysis through tensometric measurements was performed using the modern data acquisition (DAQ) system QuantumX MX840B (HBM) to receive signals from type 3/120LY11 electrical resistance strain gauges (HBM). The strain gauges are formed of two Wheatstone quarter bridges, which are then connected to the QuantumX system via two measuring channels. Quarter bridges consist of an active strain gauge and a compensating, i.e., inactive, strain gauge of the same type (Figure 7).

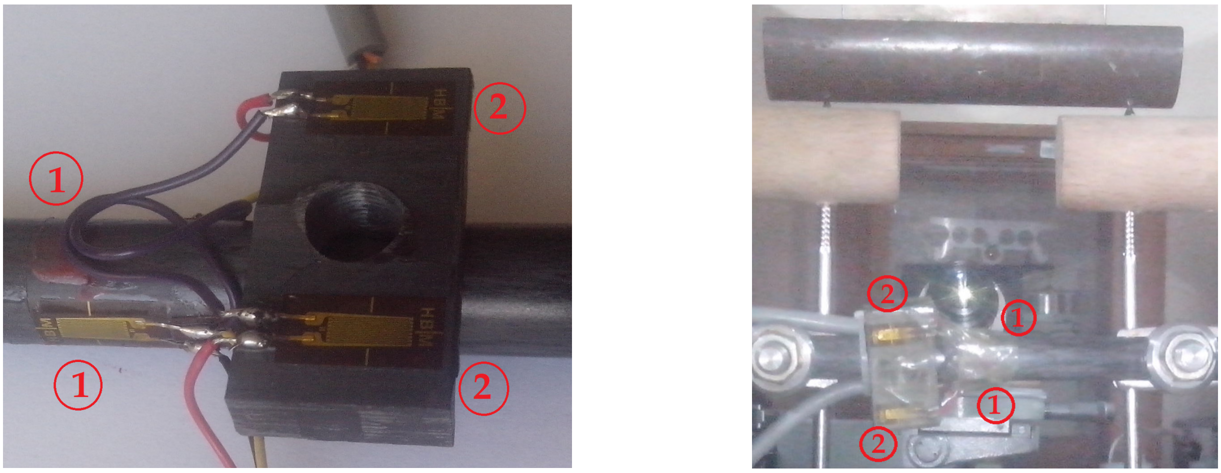

(**a**) (**b**)

Figure 7. Strain gauge arrangement; 1—active strain gauges; 2—compensation strain gauges; (**a**) mounting, (**b**) experiment.

Active strain gauges are placed on the opposite sides of the middle of the truss at the closest (MM−) and farthest (MM+) places from the bone model (Figure 7), in such a way that their longitudinal axis coincides with the direction of the maximum main deformation, that is, with the direction of the largest and smallest of the main stress at the measurement points. The previously performed structural analysis determined the direction and intensity of the main stresses at the measurement locations. Compensation strain gauges are used for temperature compensation and are of the same type as active ones. They are placed on a plate that is tied to the truss near the active strain gauges (Figure 7). The plate and the stem of the fixator are made of the same composite material. Active and compensatory strain gauges are protected from possible mechanical damage with adhesive tape after gluing. The deformation registered by the used Wheatstone bridge is given by the relation [31]

$$\varepsilon = \frac{4}{K_t}\frac{V_0}{V_S} \tag{5}$$

where V_0 and V_s are the input and output voltage of the Wheatstone bridge and K_t is the strain gauge factor.

Based on the known deformations (ε_1 and ε_3) at the measuring points and the known modulus of elasticity of the fixator frame material, using Hooke's law for the uniaxial stress state, we can determine the intensities of the main stresses at the measuring points:

$$\sigma_1 = \varepsilon_1 E;\ \sigma_3 = \varepsilon_3 E \tag{6}$$

DAQ software Catman (HBM) was used for the acquisition, monitoring and processing of measurement results from the QuantumX system.

5. Results

Comparative diagrams of point displacement at the load point of the Sarafix fixator (configuration C50) with a frame made of composite material, obtained through structural analysis using FEM and experimental testing, are shown in Figure 8.

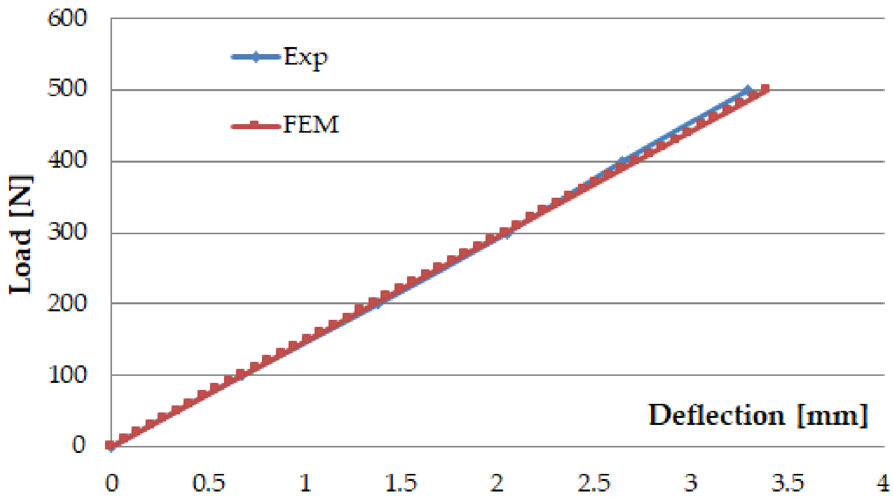

Figure 8. Comparative diagram of the deflection at the point of load for configuration C50.

From Figure 8, we can see that the deviations of the results of deflection values, obtained through FEM analysis of the results of experimental tests, amount to 2.9%, which is within the limit of permissible deviations, considering the complexity of the analyzed structure.

Also, the deviation of the results of the main stresses σ_1 MM+ and σ_3 MM− during loading from AP bending during the experimental testing and structural analysis of the C50 fixator configuration (Figure 9) amounts to a maximum of 9.5% for the main stress σ_1 on the frame of the fixator made of composite material, which is within the limit of permitted deviations, considering the complexity of the analyzed structure. The results of the displacements, as well as the main stresses for the case of other fixator configurations with different frame materials, are presented in Table 2, where one can notice a fairly good match between the results obtained through structural analysis and experimental testing. The results of the tensometric measurements of the value of the largest and smallest main stress at the center of the truss of the analyzed fixer designs are shown in Figure 10.

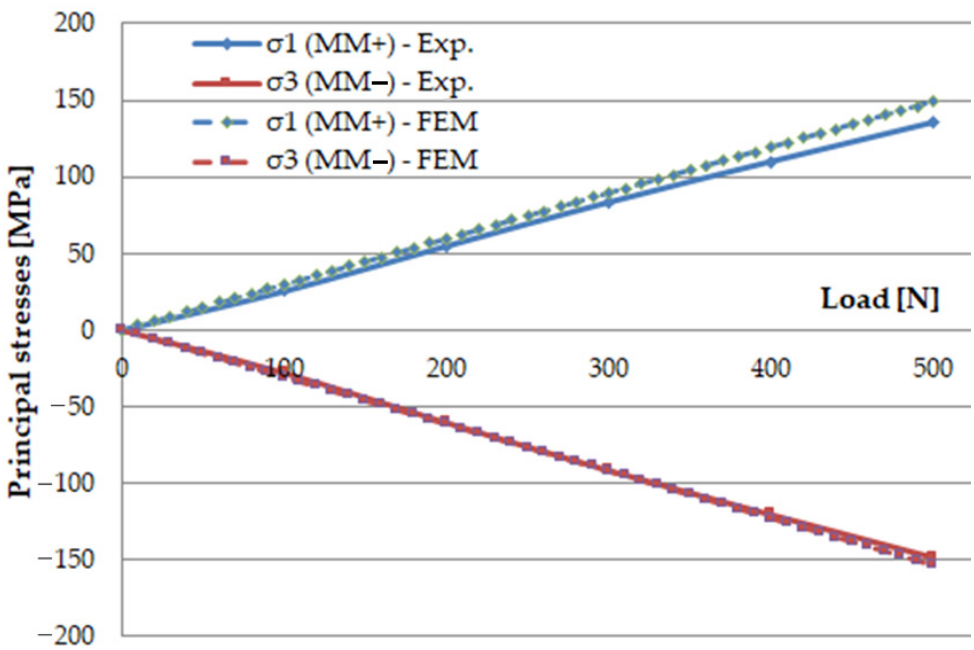

Figure 9. Comparative diagram of the principal stresses (σ_1 on MM+) and (σ_3 on MM−) for configuration C50.

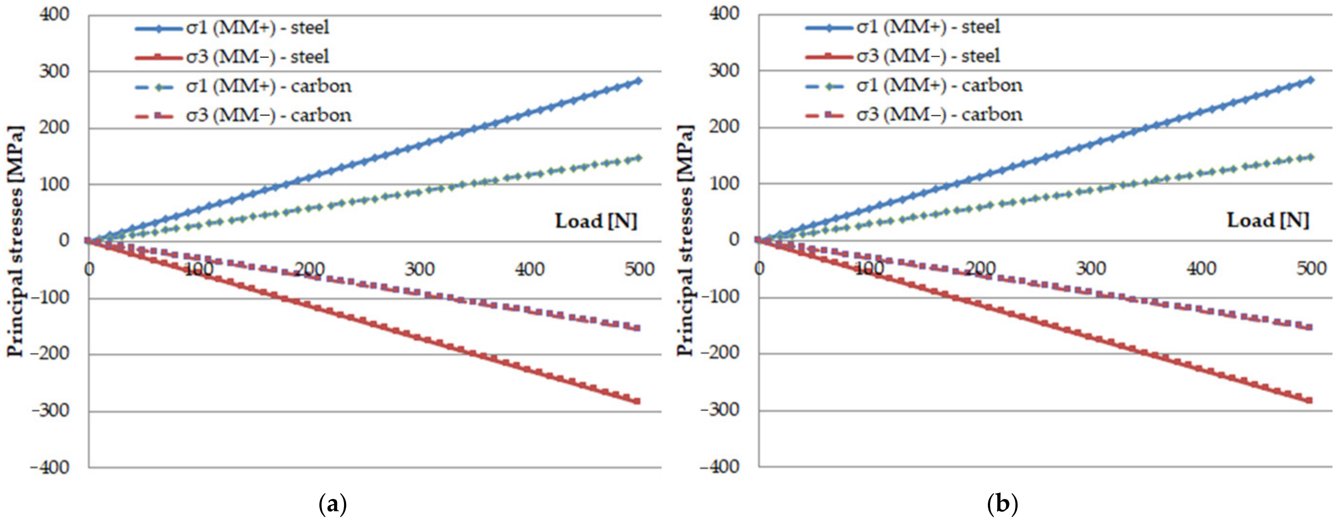

Figure 10. Values of the principal stresses due to AP bending; (**a**) B50, (**b**) C50.

The results of measuring the displacement of the bone model segments at the fracture site for the Sarafix fixator with the composite frame are shown in Figures 11 and 12. The displacements of the bone model segments at the fracture site were monitored in the direction of the x and z axis. The results of the displacement of the bone model segments at the fracture site for the case of other fixator configurations with different frame materials are shown in Table 2.

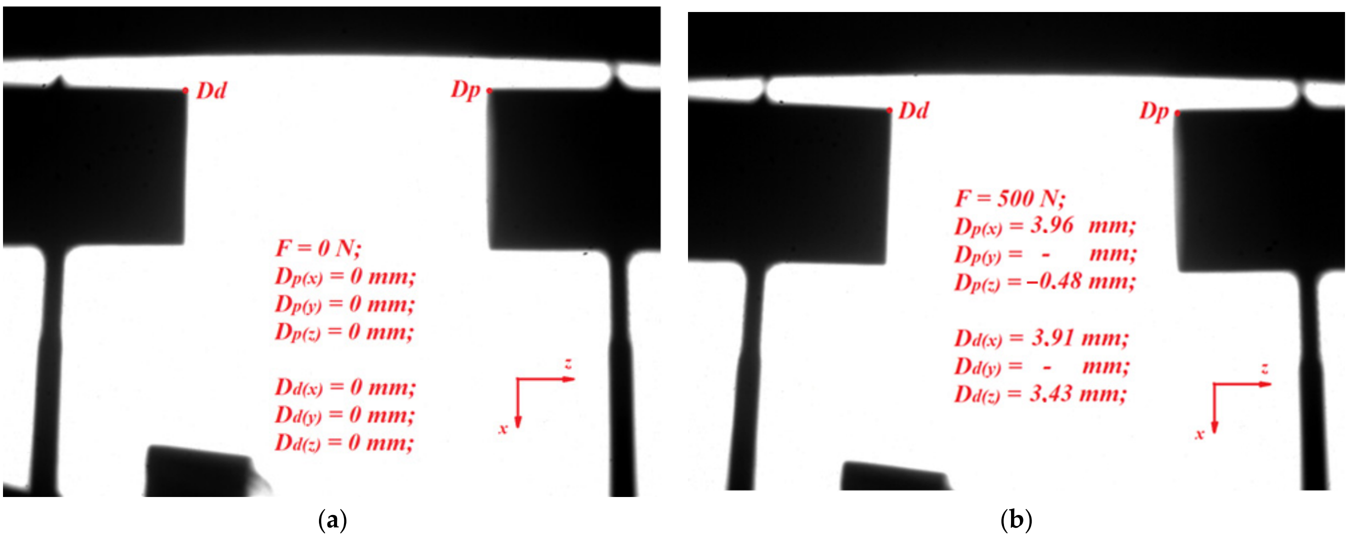

Figure 11. Displacement at the site of fracture for configuration B50; (**a**) F = 0 N, (**b**) F = 500 N.

Based on the displacement of the bone model segments at the fracture site, using Expression (3), the relative displacements of the analyzed endpoints of the proximal and distal segments ($r_{(D)x}$, $r_{(D)y}$ and $r_{(D)z}$) were determined, for which the relative displacement vector at the point of fracture (R) has a maximum value. When analyzing the stiffness of the structure (Cs) of the Sarafix fixator, the movement of the point at the point of load in the direction of the x-axis (δs) was observed (Figure 4). The results of the fixator test due to the maximum load value from AP bending Fs = 500 N are shown in Table 2.

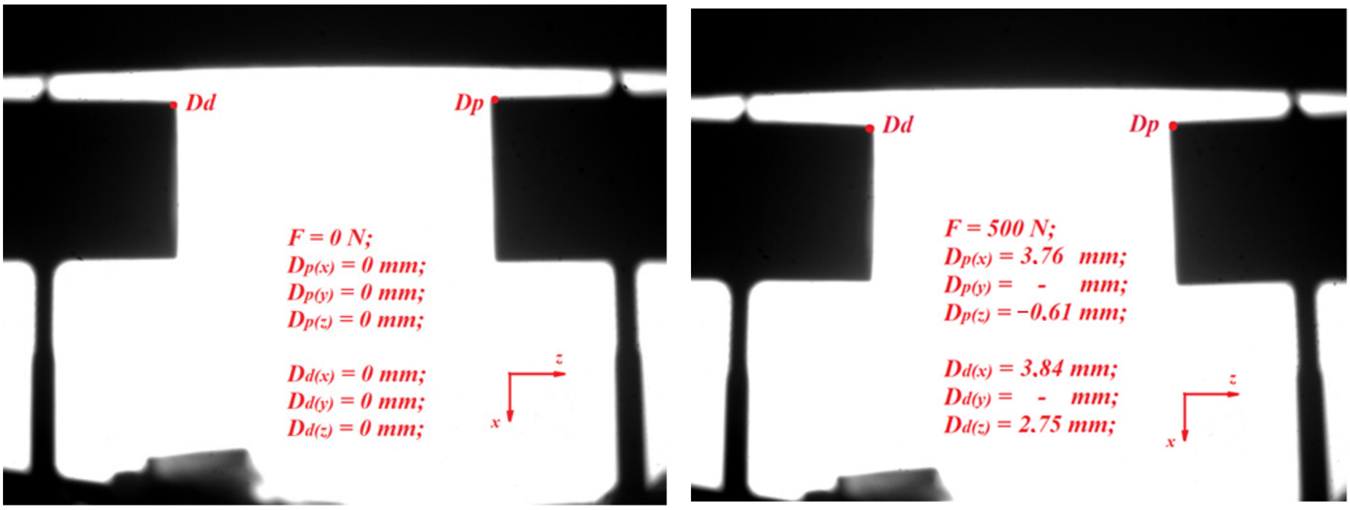

Figure 12. Displacement at the site of fracture for configuration C50; (**a**) F = 0 N, (**b**) F = 500 N.

6. Discussion

When designing and constructing external fixators, anatomical and biomechanical factors should be taken into account. From a biomechanical point of view, fracture fixation should have sufficient stability, which means a reduction in interfragmentary movement caused by external loads and muscle activity. In this paper, a comparative analysis of the biomechanical performance of the Sarafix external fixator was performed, which aimed to quantify the mechanical behavior of the fixator under the load from anterior–posterior bending for different frame materials, as well as different configurations of the fixator. Analyzing the results of displacement at the point of load from the perspective of the fixator configurations, we can notice that we have a slight difference in the values of displacement, i.e., both analyzed versions of the fixator B50 and C50 show almost equal values of displacement at the point of load. However, if we analyze the results of displacement at the load point from the perspective of the material of the fixator frame, then it can be seen that the fixator with a carbon frame has significantly higher displacements compared to the fixator with a steel frame, in the amount of up to 37% (for both configurations B50 and C50). Comparing the results of the transverse displacement of the ends of the bone segments at the fracture site from the perspective of fixator configurations, we can state that the B50 version has smaller displacement values than the C50 configuration in the case of the steel frame, in the amount of 5%, while in the case of the carbon frame, we have the opposite situation, i.e., the C50 configuration has smaller displacement values than the B50 configuration by the same amount as the steel frame case.

Analyzing the results of the transverse movements of the ends of the bone segments at the fracture site from the perspective of the fixator frame material, we can notice that the fixator with a carbon frame has greater displacements at the fracture site compared to the fixator with a steel frame, in the amount of up to 45% (for configuration B50) or up to 31% (for configuration C50). The stiffness values of the designs of the fixator were determined based on the displacement of the point at the point of loading, while the stiffness values of the fracture were determined based on the relative displacement of the analyzed pair of points of the bone segments at the fracture site (Figure 4). In the absence of major rotations, deformations, sliding joints, and plastic deformation of the fixator frame components, which is the basic requirement in terms of preserving the anatomical reduction in bone fragments in postoperative load conditions, the conducted research showed that there is a linear dependence between the load and the displacement of the bone segments, identically to the case of loading of the fixator to axial pressure [19]. Based on the anterior–posterior bending tests, we can note that both analyzed versions of the fixator B50 and C50 (for both frame materials) show almost equal values of structural stiffness and ensure similar fracture stiffness. This means that the influence of placing two half-pins in a plane at 45° to the AP plane and their distance from the load point did not significantly affect the reduction in the values of the analyzed stiffnesses according to AP bending. Also, the difference in stiffness between the B50 and C50 versions is expressed to a lesser extent than in the case of the fixator loading on axial pressure [19]. Analyzing the stiffness results from the perspective of the fixator frame material, we notice that the stiffness of the structure for both test configurations of the fixator is lower in the fixator with a carbon frame compared to the fixator with a steel frame by up to 27%. Also, we have a reduction in fracture stiffness in the amount of up to 31% (for the B50 configuration) or up to 24% (for the C50 configuration). Similar differences in stiffness between the B50 and C50 versions are only expressed to a lesser extent in the case of axial pressure loading of the fixator [19]. Based on the research conducted on the selected design versions of the Sarafix fixator, it can be established that the position of the half-pins has a negligible effect on the stability of the external fixation system in both configurations of the fixator. Observing the values of the main stresses at the control points, we can notice that with the fixator with a steel frame, we have identical stress values at both control points, for both configurations of the fixator, while with the fixator with a carbon frame, we have a slight difference in the stress values, where at the measuring point MM−, a higher stress value was measured compared to the measuring point MM+, in the amount of 5%. On the other hand, we can notice that the fixator with a carbon frame has lower stresses at critical points in the construction compared to the fixator with a steel frame, in the amount of up to 49% (at the measuring point MT+) or up to 46% (at the measuring point MT−) for both fixture test configurations. Similar differences in stress, only expressed to a lesser extent, are present in the case of axial pressure loading of the fixator [19]. Similar to the case of stiffness and stress, the research did not record a significant influence of the position of the half-pins on the stresses generated at the measuring points for either of the fixator configurations.

7. Conclusions

By analyzing the biomechanical characteristics of the fixator, it was established that:

- the configuration of the fixator with a carbon frame shows better performance only in the case of stress in critical points of the structure, i.e., it has lower stress compared to configurations with a steel frame;
- the configuration of the fixator with a carbon frame shows worse performance in terms of biomechanical characteristics, i.e., it has larger movements both at the place of loading and at the place of fracture, which, in this case, are on the border of clinically required movements;
- as a result of larger displacements in the configurations of the fixator with a carbon frame, we have less stiffness of the structure, that is, the fracture compared to the configuration of the fixator with a steel frame;
- based on the performed research, we can conclude that the configurations of the fixator with a steel frame are superior to the configurations of the fixator with a carbon frame, and the reason for this can be found in the fact that the composite material used has weaker mechanical characteristics than stainless steel.

Author Contributions: Conceptualization, N.P.; methodology, E.M. (Elmedin Mešić); software, N.P. and E.M. (Enis Muratović); validation, A.J.M. and M.D.; formal analysis, N.P.; investigation, N.P. and E.M. (Elmedin Mešić); resources, M.D.; data curation, A.J.M.; writing—original draft preparation, N.P.; writing—review and editing, E.M. (Elmedin Mešić); visualization, E.M. (Enis Muratović); supervision, A.J.M. and M.D.; project administration, N.P.; funding acquisition, N.P. All authors have read and agreed to the published version of the manuscript.

Funding: This research was funded by the Federal Ministry of Education and Science of the Federation of Bosnia and Herzegovina (grant number: 05-35-2122-1/22).

Institutional Review Board Statement: Not applicable.

Informed Consent Statement: Not applicable.

Data Availability Statement: The data underlying this study will be available on reasonable request to the corresponding author.

Conflicts of Interest: The authors declare no conflict of interest.

References

1. Remiger, A.R. Mechanical Properties of the Pinless External Fixator on Human Tibiae. *Br. J. Accid. Surg. Inj.* **1992**, *23*, 28–43. [CrossRef]
2. Grubor, P.; Mitković, M.; Tanjga, R. Značaj biomehaničkih karakteristika spoljnjeg fiksatora u liječenju kominutivnih preloma i koštanih defekata. *Acta Fac. Med. Naiss.* **2002**, *19*, 211–221.
3. Yang, L.; Saleeh, M.; Nayagam, S. The effects of different wire and screw combinations on the stiffness of a hybrid external fixator. *Proc. Inst. Mech. Eng. Part H J. Eng. Med.* **2000**, *214*, 669–676. [CrossRef] [PubMed]
4. Vossoughi, J.; Youm, Y.; Bosse, M.; Burgess, A.R.; Poka, A. Structural stiffness of the Hoffmann simple anterior tibial external fixation frame. *Ann. Biomed. Eng.* **1989**, *17*, 127–141. [CrossRef]
5. Meleddu, A.; Barrault, S.; Zysset, P.K. A Rigorous Method for Evaluation of the 6D Compliance of External Fixators. *Biomech. Model. Mechanobiol.* **2006**, *6*, 253–264. [CrossRef] [PubMed]
6. Oh, J.K.; Lee, J.J.; Jung, D.K.; Kim, B.J.; Oh, C.W. Hybrid External Fixation of Distal Tibial Fractures: New Strategy to Place Pins and Wires without Penetrating the Anterior Compartment. *Arch. Orthop. Trauma Surg.* **2004**, *124*, 542–546. [CrossRef]
7. Radke, H.; Aron, D.N.; Applewhite, A.; Zhang, G. Biomechanical Analysis of Unilateral External Skeletal Fixators Combined with IM-Pin and without IM-Pin Using Finite-Element Method. *Vet. Surg.* **2006**, *35*, 15–23. [CrossRef]
8. Ramakrishna, S.; Mayer, J.; Wintermantel, E.; Leong, K.W. Biomedical applications of polymer-composite materials: A review. *Compos. Sci. Technol.* **2001**, *61*, 1189–1224. [CrossRef]
9. Salernitano, E.; Migliaresi, C. Composite materials for biomedical applications: A review. *J. Appl. Biomater. Biomech.* **2003**, *1*, 3–18.
10. Pervan, N.; Mesic, E.; Colic, M.; Avdic, V. Stiffness Analysis of the Sarafix External Fixator based on Stainless Steel and Composite Materials. *TEM J.* **2015**, *4*, 366–372.
11. Gibson, R.F. *Principles of Composite Material Mechanics*, 4th ed.; CRC Press: Boca Raton, FL, USA, 2016.
12. Baidya, K.P.; Ramakrishna, S.; Rahman, M.; Ritchie, A.; Huang, Z.M. An Investigation on the Polymer Composite Medical Device—External Fixator. *J. Reinf. Plast. Compos.* **2003**, *22*, 563–590. [CrossRef]
13. Lee, M.G.; Chung, K.; Lee, C.J.; Park, J.H.; Kim, J.; Kang, T.J.; Youn, J.R. The viscoelastic bending stiffness of fiber-reinforced composite Ilizarov C-rings. *Compos. Sci. Technol.* **2001**, *61*, 2491–2500. [CrossRef]
14. Fu, T.; Zhao, J.L.; Xu, K.W. The designable elastic modulus of 3-D fabric reinforced biocomposites. *Mater. Lett.* **2007**, *61*, 330–333. [CrossRef]
15. Saidpour, S.H. Assessment of Carbon Fibre Composite Fracture Fixation Plate Using Finite Element Analysis. *Ann. Biomed. Eng.* **2006**, *34*, 1157–1163. [CrossRef] [PubMed]
16. Zahra, S.B.; El Sawi, I.; Emil, H.S.; Rad, Z.; Habiba, B. Biomechanical properties of an advanced new carbon/flax/epoxy composite material for bone plate applications. *J. Mech. Behav. Biomed. Mater.* **2013**, *20*, 398–406.
17. Dozic, S.; Salihefendic, R.; Baralic, E.; Fazlagic, S.; Djikic, S.; Basic, S.; Kulenovic, F. Sarafix external fixator in the treatment of war-related extremity injuries at Sarajevo State Hospital during the period May 1992–May 1995. In Proceedings of the First Congress of War Surgery, Sarajevo, Bosnia and Herzegovina, 12–15 May 1996.
18. Djozic, S.; Shetty, A.A.; Hansen, U.; James, K.D. *Biomechanical Test Results of the Sarafix—External Fixator*; Imperial College: London, UK, 2004.
19. Pervan, N.; Mešić, E.; Muminović, A.J.; Delić, M.; Muratović, E.; Trobradović, M.; Hadžiabdić, V. Biomechanical Performance Analysis of the Monolateral External Fixation Devices with Steel and Composite Material Frames under the Impact of Axial Load. *Appl. Sci.* **2022**, *12*, 722. [CrossRef]
20. Naylor, A. Can Wood be used as a Bio-mechanical Substitute for Bone during Evaluation of Surgical Machining Tools? *BioResources* **2014**, *9*, 5778–5781. [CrossRef]
21. Mešić, E.; Pervan, N.; Muminović, A.J.; Muminović, A.; Čolić, M. Development of Knowledge-Based Engineering System for Structural Size Optimization of External Fixation Device. *Appl. Sci.* **2021**, *11*, 10775. [CrossRef]
22. Li, J.; Zhao, X.; Hu, X.; Tao, C.; Ji, R. A theoretical analysis and finite element simulation of fixator–bone system stiffness on healing progression. *J. Appl. Biomater. Funct. Mater.* **2018**, *16*, 115–125. [CrossRef]
23. Koo, T.K.; Chao, E.Y.; Mak, A.F. Fixation Stiffness of Dynafix Unilateral External Fixator in Neutral and Non-neutral Configurations. *Bio-Med. Mater. Eng.* **2005**, *15*, 433–444.
24. Claes, L.; Laule, J.; Wenger, K.; Suger, G.; Liener, U.; Kinzl, L. The Influence of the Stiffness of the Fixator on Maturation of Callus after Segmental Transport. *J. Bone Jt. Surg.* **2000**, *82*, 142–148. [CrossRef]
25. Pervan, N.; Muminović, A.J.; Mešić, E.; Delić, M.; Muratović, E. Analysis of Mechanical Stability for External Fixation Device in the Case of Anterior-Posterior Bending. *Adv. Sci. Technol. Res. J.* **2022**, *16*, 136–142. [CrossRef]
26. Pervan, N.; Muminović, A.J.; Mešić, E.; Muratović, E.; Delić, M. Analysis of the Mechanical Behaviour for the External Fixation Device under the Impact of Torque. *Teh. Glas.* **2023**, *17*, 20–25.

27. Pervan, N.; Mešić, E.; Muminović, A.J.; Delić, M.; Muratović, E. Stiffness Analysis of the External Fixation System at Axial Pressure Load. *Adv. Sci. Technol. Res. J.* **2022**, *16*, 226–233. [CrossRef]
28. Mesic, E.; Avdic, V.; Pervan, N.; Repcic, N. Finite Element Analysis and Experimental Testing of Stiffness of the Sarafix External Fixator. *Procedia Eng.* **2015**, *100*, 1598–1607.
29. Mesic, E.; Avdic, V.; Pervan, N. Numerical and experimental stress analysis of an external fixation system. *Folia Medica Fac. Med. Univ. Saraev.* **2015**, *50*, 52–58.
30. Mešić, E.; Muminović, A.; Čolić, M.; Petrović, M.; Pervan, N. Development and Experimental Verification of a Generative CAD/FEM Model of an External Fixation Device. *Teh. Glas.* **2020**, *14*, 1–6. [CrossRef]
31. Mesic, E.; Pervan, N.; Repcic, N.; Muminovic, A. Research of Influential Constructional Parameters on the Stability of the Fixator Sarafix. In Proceedings of the 23rd International DAAAM Symposium, Zadar, Croatia, 24–27 October 2012; pp. 561–564.